CFSRC COLLOQUIUM

Proceedings of the Cold-Formed Steel Research Consortium Colloquium
17-19 October 2022 (cfsrc.org)

Design of Cold-Formed Steel Built-Up Closed Section Columns - Modified Local Slenderness Equation

Sivaganesh Selvaraj[1], Mahendrakumar Madhavan[2]

Abstract

Structural behavior of Cold-formed Steel (CFS) face-to-face connected built-up closed cross-section columns is investigated. The CFS built-up columns are designed as long and locally slender to verify the influence of intermediate longitudinal connection spacing and check the appropriateness of the current Direct Strength Method (DSM) design and the intermediate connection spacing limitations of AISI. A total of 31 axial compression tests were carried out with fixed-fixed end conditions. The design parameters such as local slenderness, global slenderness, intermediate longitudinal fastener spacing, and length of the column are varied. The failure modes of the column are summarized and the reason for them is explained. The influence of intermediate longitudinal connection spacing was observed in the ultimate loading capacity and failure modes. The test results including ultimate load and failure modes were compared with the current direct strength method design predictions. A modified local slenderness expression is proposed to consider the influence of intermediate longitudinal fastener spacing in the design strength of cold-formed steel built-up closed cross-section columns.

1. General

Cold-formed Steel is rapidly becoming a common construction material since it has a wide range of applications owing to its highly efficient nature (strength to weight ratio and feasibility for the fabrication of optimized cross-sections). Cold-formed steel structural members are typically open cross-sections, being used as beams, columns, joists, wall studs, purlins, rafters and in some instances as scaffolding structures. However, the design efficiency of the CFS structural member starts waning when the structure requires a long member with no provision for bracings. In addition, the need of long members makes it vulnerable to instability failures due to high slenderness and open cross sections [1-3]. The instability failure of CFS structural members can be prevented by transforming the open cross-sections (higher slenderness) into closed ones (reduced slenderness). The closed cross-sections have high torsional rigidity and less vulnerable to failure in collapsible failure modes [4-6].

Though it is practically feasible to manufacture and use CFS closed cross-sections for construction [7], the expression for predicting the design strength of such built-up members is currently unavailable. Several researchers in the past have attempted to modify the current design method of AISI [8], Eurocode [9] and AS/NZS [10] which are based on the structural behavior of CFS open cross-sections. However, the development of such design provisions are still in the nascent stage [11-16]. The impediment to the development of a robust design expression is due to the inability to accurately predict the influence of intermediate longitudinal fastener spacing and interactive failure modes such as local-global, local-distortional, distortional-global, and flexural torsional buckling interacting with local and distortional buckling. The influence of these failure modes in the design strength of various CFS closed cross-section was not fully studied.

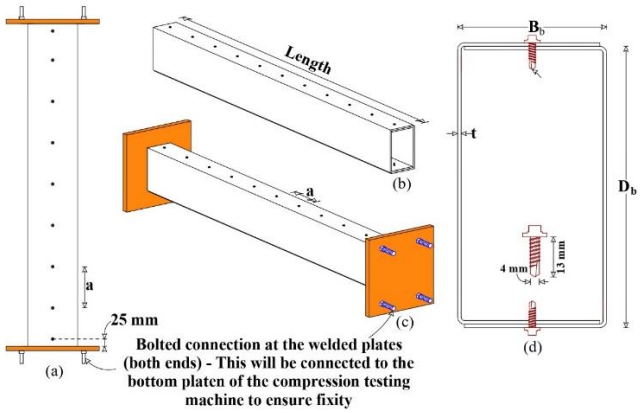

Fig. 1. Cold formed steel face-to-face connected built-up columns: (a) Full View of the Built-up column; (b) 3D view of the column; (c) 3D view of the column with base plates; (d) Dimensions of the CFS built-up column cross-section

[1] Postdoctoral fellow, Department of Civil and Environmental Engineering, The Hong Kong Polytechnic University, Hong Kong. sivaganesh.selvaraj@polyu.edu.hk
[2] Professor, Department of Civil Engineering, Indian Institute of Technology Hyderabad, Telangana, India. mkm@ce.iith.ac.in

The present study endeavors to investigate the structural behavior of CFS face-to-face connected long and locally slender columns with an influence of intermediate longitudinal fastener spacing (Fig. 1). An experimental investigation on CFS closed built-up cross-sections with various local slenderness, global slenderness, intermediate longitudinal fastener spacing, and length of the column was carried out in the present study. The experimental results were compared with the current design specifications of AISI S100 [8]. An appropriate modification in design to incorporate the influence of intermediate longitudinal fastener spacing (a) is suggested. The conclusion from this study will be beneficial for further investigation on the structural behavior of CFS built-up columns and assessment of AISI S100 design expressions. The experimental test-setup, material properties, geometric imperfection data and detailed failure mode investigations are presented in Selvaraj and Madhavan [17-19]

2. Test results and discussion

The ultimate compression strengths and failure modes of the CFS built-up face-to-face closed cross-section columns with different cross-sectional dimensions, slenderness ratios, and intermediate longitudinal fastener spacings were investigated in the experiments. The column test results (P_{TEST} and failure modes) are summarized in Table 1. The axial deformation vs axial compression load plots for the built-up column tests are shown in Figs. 2-5 with their corresponding failure modes. The failure load P_{TEST} is the ultimate load of each built-up column obtained from the tests and the corresponding failure modes are observed at ultimate loads. Though the columns are designed to be long (L > 20r), all the columns failed in local buckling as can be observed in Failure mode Figures (Fig. 6-10). In addition, the visual observation on the failure modes and interpretation of the test results indicated that there was no local-global interaction buckling in the tested columns. It is observed that the intermediate longitudinal fastener spacing (a) influenced the failure modes and strengths of the face to face connected long columns significantly. A more detailed discussion about the structural behaviour and failure modes including Integrity of the face-to-face connected built-up columns and Failure mode - Perception of reality is described in [18].

3. Local buckling pattern in face-to-face Built-up columns

Local buckling waves were observed in the entire length of the specimen from the initial stage of loading as shown in Fig. 2, with the amplitude of the wave becoming more pronounced as the load approached the ultimate compressive strength. Later, the specimens failed in local buckling followed by decrease in load. After unloading, the magnitude of the local buckling waves gradually decreased as can be observed by comparing the failure mode photos at ultimate load and after-test of the locally buckled specimens (Fig. 3). Finally, an unrecoverable plastic yield zone was observed in one side flange of the CFS built-up cross-section as shown in Figs. 3 (after test photos). The difference in plastic yield zone locations between the same set of specimens may be attributed to differences in the initial flare imperfections and intermediate longitudinal fastener spacing.

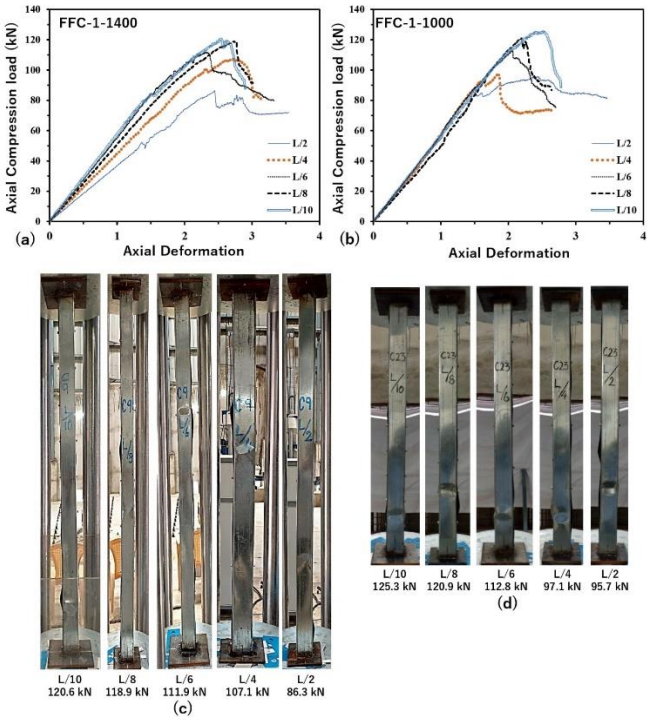

Fig. 2. Experimental results - Load displacement plot and failure modes: (a and c) FFC-1-1400 built-up column; (b and d) FFC-1-1000 built-up column

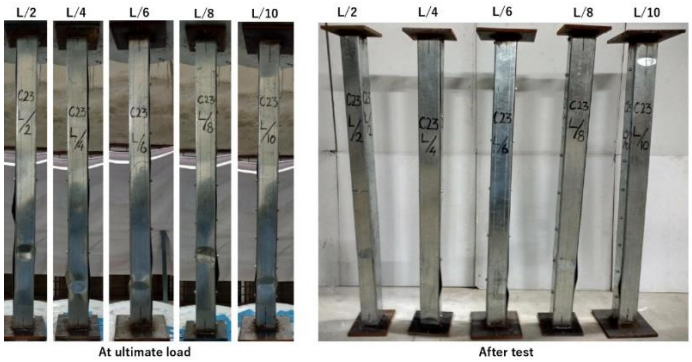

Fig. 3. Failure modes picture of FFC-1-1000 built-up column: (a) Failure mode at ultimate load; (b) Failure mode after releasing the load - Recovery of local buckling in the Built-up columns and presence of plastic yield zone

Fig. 4. Local buckling Failure mode pattern in face-to-face connected built-up columns

The local buckling occurred in both webs and flanges of the CFS built-up cross-section as shown in Fig. 2. It should be noted that the local buckling in the flanges occurred only in between the fastener spacing (Figs. 4 and 5b). The nature of the local buckling in flanges of individual CFS structural members is symmetrical on both flanges (either outward-outward or inward-inward) as shown in Fig. 5a. It should be further noticed from Fig. 5a that when the web buckles inward the flanges try to buckle outwards and while the web buckles outwards the flange tries to buckle inward to maintain the 90-degree angle corner. Such symmetrical local buckling on the flanges of the CFS structural members was observed in the previous literature [20 - 27]. However, the occurrence of local buckling in the built-up member is different. The possible local buckling failure modes in the face-to-face connected built-up columns are shown in Fig. 5(b-f). The possible local buckling modes are defined as follows: (i) Webs buckling inward and the flanges try to buckle outwards, wherein only the outer flanges can buckle freely while the inner flanges are restrained due to over lapping effect (Fig. 5c); (ii) Webs buckling outwards and the flanges try to buckle inwards; in this failure mode only the inner flanges can buckle freely while the outer flanges are restricted due to overlapping effect (Fig. 5d); (iii) Local buckling at the fastener connection location: one web is buckling inward and the other web is buckling outward but the flange buckling is restrained due to the fastener connection (Fig. 5e); (iv) one web is buckling inward and the other web is buckling outward, the outward buckling of web causes inward flange buckling and similarly inward web buckling causes outward flange buckling. However, due to the built-up cross-section pattern (flanges overlapping each other) both the flanges on only one side are free to buckle, while on the other side the flange local buckling is restrained since the flange displacements are towards each other as shown in Fig. 5f.

Theoretically, both the flanges of the built-up cross-sections are considered as unstiffened, however, practically the flanges will be subjected to partial restraint from adjacent flange due to overlapping. Therefore, only one flange among the overlapped flanges will be free to buckle locally as shown in Figs. 5c, 5d, and 5f. This failure mode can be further explained as follows. The face-to-face built-up specimens are formed by locking two channels together with overlapping flanges. At one side, the first flange overlaps the second flange and at the other side, the second flange overlaps the first flange (Fig. 1d). Due to this, the natural symmetrical local buckling (inward-inward or outward-outward) on both the flanges is not possible. The failure mode shown in Fig. 4 depicts the local buckling failure of the CFS built-up column where it can be observed that there is no symmetry in local buckling due to the overlapping of flanges. From Figure 4 it can be observed that in the front view the local buckling can be seen in Side A (Channel 2) while in the back view the local buckling can be seen in Side B (Channel 1), indicating that one of the flanges is subjected to overlapping restraint.

3.1 Influence of Interconnection spacing in local buckling stress

Though it is clear that the face-to-face connected built-up columns failed in local buckling, it should be noted that there is a significant difference in the strength and stiffness between the built-up columns with different intermediate longitudinal fastener spacing (a) (Fig. 2 and Table 1). This difference between the strength and stiffness shall be attributed to the resistance offered by the fastener connections and restraint from flange overlap for local buckling. The amount of influence of fastener connections on the local buckling strength can be determined by comparing the actual stress of the built-up column from the experimental data and theoretical local buckling stress (F_{TEST}/F_{crl}). The ratio of F_{TEST}/F_{crl} for all the test results is shown in Table 1. The F_{TEST}/F_{crl} ratios are mostly higher than unity, ranging from 1 to 2.17, indicating that the actual buckling stress (F_{TEST}) is always higher than the theoretical local buckling stress (F_{crl}). The improvement in actual local buckling stress with respect to the intermediate longitudinal fastener spacing (a) is presented in Fig. 6. As the a/L_{crl} ratio decreases the influence of overlap increases [increase in

actual buckling stress (F_{TEST}) compare to the theoretical load (F_{cre})]. The reason for the improvement in the local buckling stress may be attributed to the restraints provided due to overlapping by either one of the flanges on the other. The influence of flange overlap is significant when the a/L_{crl} ratio is smaller than 4 and closer to 1 as can be seen in Fig. 6. Further, the influence of intermediate longitudinal fastener spacing on the design strength of CFS built-up columns is discussed in the later sections.

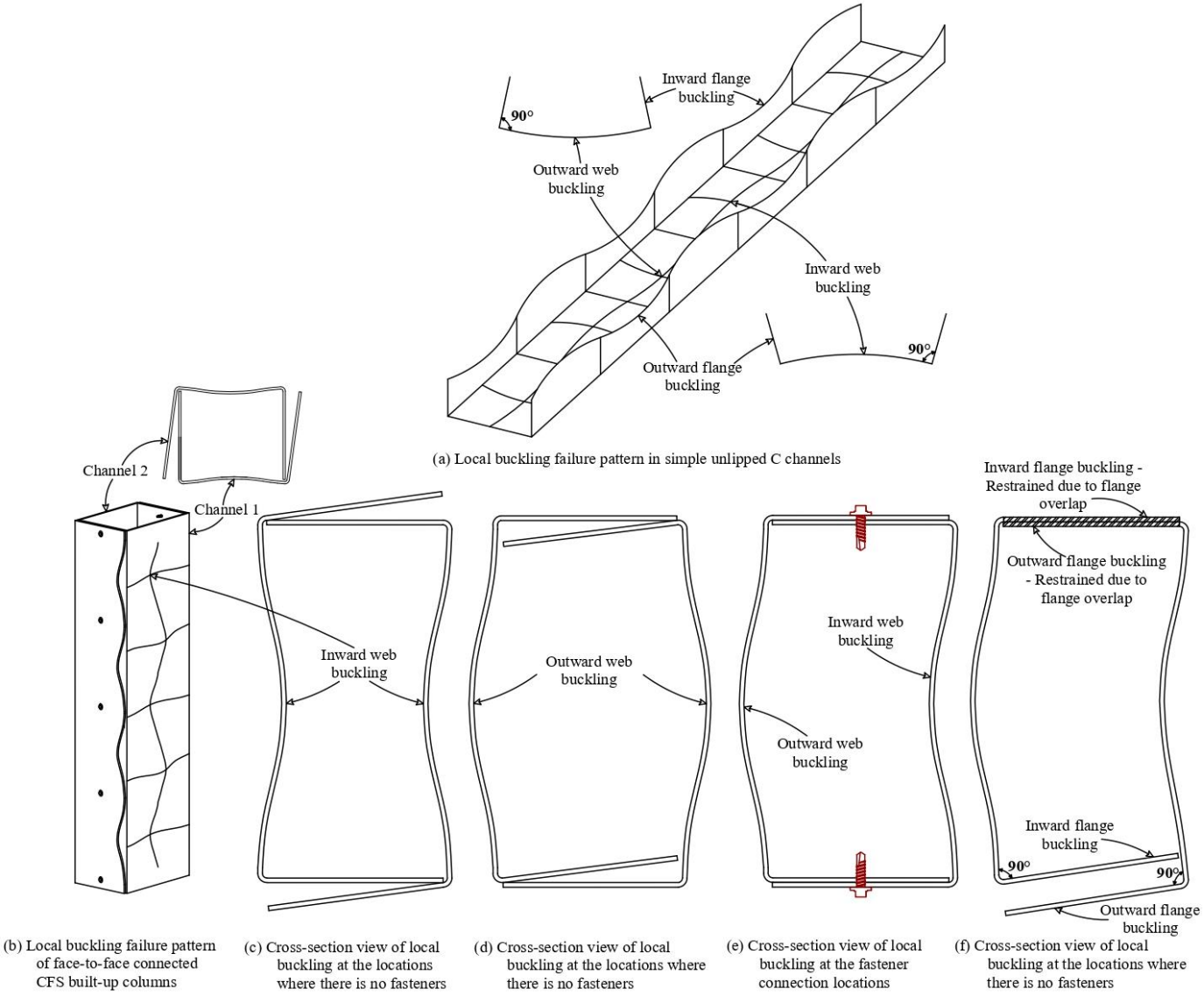

Fig. 5. Possible local buckling failure modes in built-up columns and restrained due to the flange overlapping

4.Current Design Method for CFS Axial Compression Structural Members (PDSM)

Currently, there is no explicit design provision for the design of CFS built-up members, except the modified global slenderness approach of AISI [8]. The AISI recommends using the modified global slenderness expression to include the effect of intermediate longitudinal fastener spacing (a) in the design strength of CFS built-up columns. The direct strength method (DSM) for the design of CFS structural members with conventional shapes has been now included in the main specification of AISI S100 [8]. The present study evaluates the appropriateness of the direct strength method of AISI S100 [8] with the modified global slenderness expressions (KL/r_m) for the design of built-up closed section columns using the experimental results.

The nominal compression strength of the CFS column member (P_{DSM}) should be the minimum of the nominal global buckling strength (P_{ne}) and local buckling strength (P_{nl}) as per the following equations

Table 1. Slenderness and Test results of Face-to-Face connected Cold-formed steel built-up columns

Specimen	Slenderness		Fastener Spacing (a)	L_{crl}	(a/r) / (KL/r)	Experimental results		
	λ_l	λ_c				P_{TEST} (kN)	F_{cre} / F_{TEST}	F_{TEST} / F_{crl}
FFC-1-1400-L/10	1.719	0.49	140	140	0.23	120.59	6.44	1.91
FFC-1-1400-L/8		0.50	175	140	0.29	118.90	6.34	1.88
FFC-1-1400-L/6		0.51	233	140	0.37	111.99	6.32	1.77
FFC-1-1400-L/4		0.56	350	140	0.52	107.06	5.63	1.69
FFC-1-1400-L/2		0.75	700	140	0.77	86.31	3.88	1.36
FFC-1-1000-L/10		0.35	100	140	0.23	125.34	12.15	1.98
FFC-1-1000-L/8		0.36	125	140	0.29	120.94	12.21	1.91
FFC-1-1000-L/6		0.37	167	140	0.37	112.84	12.29	1.78
FFC-1-1000-L/4		0.40	250	140	0.52	97.07	12.17	1.53
FFC-1-1000-L/2		0.53	500	140	0.77	95.72	6.85	1.51
FFC-2-1800-L/10	1.727	0.59	180	140	0.23	120.15	4.64	1.86
FFC-2-1800-L/8		0.60	225	140	0.28	118.87	4.56	1.84
FFC-2-1800-L/6		0.61	300	140	0.36	104.81	4.87	1.62
FFC-2-1800-L/4		0.66	450	140	0.50	98.59	4.45	1.53
FFC-2-1800-L/2		0.88	900	140	0.76	77.78	3.20	1.20
FFC-3-1800-L/4	1.970	0.62	450	150	0.46	96.78	5.33	1.89
FFC-3-1800-L/2		0.79	900	150	0.72	80.18	3.95	1.57
FFC-3-1200-L/8		0.38	150	150	0.25	111.07	12.39	2.17
FFC-3-1200-L/6		0.39	200	150	0.32	91.62	14.33	1.79
FFC-4-1800-L/10	1.772	0.63	180	130	0.23	107.19	4.12	1.90
FFC-4-1800-L/8		0.64	225	130	0.29	99.00	4.33	1.76
FFC-4-1800-L/6		0.66	300	130	0.37	95.86	4.20	1.70
FFC-4-1200-L/10		0.42	120	130	0.23	111.54	8.91	1.98
FFC-4-1200-L/4		0.48	300	130	0.51	110.26	7.02	1.96
FFC-4-1200-L/2		0.64	600	130	0.77	85.87	5.03	1.52
FFC-5-1800-L/10	1.539	0.66	180	130	0.22	96.91	3.87	1.40
FFC-5-1800-L/6		0.69	300	130	0.36	83.62	4.12	1.21
FFC-5-1800-L/2		0.98	900	130	0.75	69.27	2.47	1.00
FFC-5-1000-L/10		0.37	100	130	0.22	102.86	11.81	1.48
FFC-5-1000-L/6		0.38	167	130	0.36	103.41	10.80	1.49
FFC-5-1000-L/2		0.54	500	130	0.75	80.68	6.88	1.16
						Average	6.95	1.66
						Max	14.33	2.17
						Min	2.47	1

$\lambda_c = \sqrt{P_y/P_{cre}}$; $\lambda_l = \sqrt{P_{ne}/P_{crl}}$; L = Local buckling; P_{TEST} = ultimate load of each built-up column; P_y = Yield strength of column (over all cross-sectional area multiplied by yield stress); F_{cre} = theoretical buckling stress determined according to AISI; F_{crl} = theoretical local buckling stress obtained from Thinwall; F_{TEST} = P_{TEST} / Cross-sectional area of the Built-up column; L_{crl} = Half-wave length arrived from Thinwall software.

$$P_{DSM} = \min(P_{ne}, P_{nl}) \quad (1)$$

$$P_{ne} = \begin{cases} \left(0.658^{\lambda_c{}^2}\right) P_y & if\ \lambda_c \le 1.5 \\ \left(\frac{0.877}{\lambda_c{}^2}\right) P_y & if\ \lambda_c > 1.5 \end{cases} \quad (2)$$

$$P_{nl} = \begin{cases} P_{ne} & if\ \lambda_l \le 0.776 \\ \left[1 - 0.15\left(\frac{P_{crl}}{P_{ne}}\right)^{0.4}\right]\left(\frac{P_{crl}}{P_{ne}}\right)^{0.4} P_y & if\ \lambda_l > 0.776 \end{cases} \quad (3)$$

$$\lambda_c = \sqrt{P_y/P_{cre}} \quad \lambda_l = \sqrt{P_{ne}/P_{crl}}$$

Where P_y is the yield strength (gross full built-up section area x yield stress), P_{crl} is the elastic critical local buckling load that may be obtained from Thinwall. P_{cre} is determined from multiplying F_{cre} with the gross full built-up section area.

For evaluation, the global buckling design strength (only using Eq. (2)] of CFS built-up columns using modified slenderness ratio is compared with the experimental strength in Fig. 7. Figure 7 shows that the experimental strength (P_{TEST}) is lower than the global buckling curve (P_{ne}) for all the specimens confirming once again (addition to failure modes shown in Figs. 2-3) that all the tested built-up columns failed in local buckling. The design strength (P_{DSM}) of CFS face-to-face connected built-up columns determined using Eqs. (1-3) are summarized in Table 2.

Table 2. Comparison between Test and DSM predictions

Specimen	a/L_{crl}	P_{TEST} (kN)	Local (λ_l)	P_{DSM} (kN) (Eqs. 1-3)	Local (λ_{lm}) (Eq. 5)	P_{DSM}^M (kN) (Eq. 4)	P_{TEST} / P_{DSM}	P_{TEST} / P_{DSM}^M
FFC-1-1400-L/10	1.00	120.59	1.635	102.51	1.635	102.51	1.18	1.18
FFC-1-1400-L/8	1.25	118.90	1.632	102.30	1.707	94.47	1.16	1.26
FFC-1-1400-L/6	1.67	111.99	1.627	101.86	1.802	84.77	1.10	1.32
FFC-1-1400-L/4	2.50	107.06	1.611	100.60	1.935	72.17	1.06	1.48
FFC-1-1400-L/2	5.00	86.31	1.529	94.05	2.110	52.21	0.92	1.65
FFC-1-1000-L/10	0.71	125.34	1.676	105.82	1.566	119.14	1.18	1.05
FFC-1-1000-L/8	0.89	120.94	1.674	105.71	1.637	110.05	1.14	1.10
FFC-1-1000-L/6	1.19	112.84	1.671	105.48	1.731	99.10	1.07	1.14
FFC-1-1000-L/4	1.79	97.07	1.663	104.81	1.868	85.02	0.93	1.14
FFC-1-1000-L/2	3.57	95.72	1.620	101.28	2.089	63.63	0.95	1.50
FFC-2-1800-L/10	1.29	120.15	1.606	102.36	1.689	93.58	1.17	1.28
FFC-2-1800-L/8	1.61	118.87	1.603	102.08	1.762	86.11	1.16	1.38
FFC-2-1800-L/6	2.14	104.81	1.596	101.48	1.858	77.08	1.03	1.36
FFC-2-1800-L/4	3.21	98.59	1.575	99.79	1.989	65.27	0.99	1.51
FFC-2-1800-L/2	6.43	77.78	1.468	91.10	2.130	46.10	0.85	1.69
FFC-3-1800-L/4	3.00	96.78	1.818	94.90	2.264	63.38	1.02	1.53
FFC-3-1800-L/2	6.00	80.18	1.728	88.95	2.473	45.82	0.90	1.75
FFC-3-1200-L/8	1.00	111.07	1.911	101.22	1.911	101.22	1.10	1.10
FFC-3-1200-L/6	1.33	91.62	1.909	101.03	2.022	91.01	0.91	1.01
FFC-4-1800-L/10	1.38	107.19	1.629	91.00	1.739	80.99	1.18	1.32
FFC-4-1800-L/8	1.73	99.00	1.625	90.70	1.814	74.45	1.09	1.33
FFC-4-1800-L/6	2.31	95.86	1.616	90.05	1.911	66.53	1.06	1.44
FFC-4-1200-L/10	0.92	111.54	1.707	96.63	1.680	99.42	1.15	1.12
FFC-4-1200-L/4	2.31	110.26	1.689	95.32	1.997	70.34	1.16	1.57
FFC-4-1200-L/2	4.62	85.87	1.626	90.78	2.208	51.79	0.95	1.66
FFC-5-1800-L/10	1.38	96.91	1.404	92.32	1.498	82.33	1.05	1.18
FFC-5-1800-L/6	2.31	83.62	1.393	91.35	1.646	67.80	0.92	1.23
FFC-5-1800-L/2	6.92	69.27	1.259	80.06	1.854	39.76	0.87	1.74
FFC-5-1000-L/10	0.77	102.86	1.496	100.25	1.419	109.84	1.03	0.94
FFC-5-1000-L/6	1.28	103.41	1.492	99.92	1.568	91.52	1.03	1.13
FFC-5-1000-L/2	3.85	80.68	1.446	95.96	1.894	58.92	0.84	1.37
						Mean (P_m)	1.04	1.34
						Standard Deviation	0.109	0.227
						Coefficient of variation	0.105	0.169
						Reliability analysis in accordance with the loading combinations of ASCE [30]	2.93	3.52
						Reliability analysis in accordance with the loading combinations of AZ/NZS [31]	2.98	3.54

λ_{lm} = Eq. (5); P_{TEST} = ultimate load of each built-up column; P_{DSM} = Nominal strength of column as per current AISI [Eqs. (1-3)]; P_{DSM}^M = Nominal strength of column as according to the modified local slenderness [Eqs. (4-5)];

It should be noted that the design strength (P_{DSM}) shown in Table 2 is the minimum of nominal global buckling strength [P_{ne} - Eq. (2)] and local buckling strength [P_{nl} - Eq. (3)]. The comparison of design strength (P_{DSM}) with the experimental strength indicates that the design strength predicted by the set of DSM expressions is unconservative (i.e experimental strength < design strength) for 11 of the 31 specimens tested (see P_{TEST}/P_{DSM} in Table 2) with the coefficient of variation 0.105. The unconservativeness of the current AISI DSM method is also shown in Fig. 8 and Fig. 9.

Further, the investigation on the design strength prediction indicates that the current design predictions did not accurately incorporate the effect of intermediate longitudinal fastener spacing (a). To be precise, the local slenderness [$\lambda_l = (P_{ne}/P_{crl})0.5$] of the built-up cross-section should increase due to the increase in a/L_{crl} ratio. However, due to the modified global slenderness ratio the magnitude of P_{ne} is reduced. A reduction in P_{ne} results in lower local slenderness (λ_l) consequently leading to higher P_{nl} (Eq. 3). The reduced slenderness can be compared from Table 2, where λ_l of FFC-1-1400-L/10 is 1.635 while the λ_l of FFC-1-1400-L/2 is 1.529. In addition, it should also be noted that the unconservative design predictions are only for the specimen with intermediate longitudinal fastener spacing of L/6 or higher as can be observed from Fig. 8. Moreover, the

trend in the face-to-face connected built-up columns indicates a significant decrease in load as the a/L_{crl} magnitudes increases (Figs. 6 and 9). In contrast, as the a/L_{crl} ratio decreases the strength of the built-up column increases due to the restraint provided by the fastener connection and flange overlapping, particularly for a/L_{crl} ratio less than 2 as shown in Fig. 9. Therefore, the current design expressions of AISI should be modified to increase the local buckling strength when the a/L_{crl} ratio is less and decrease the local buckling strength when the a/L_{crl} ratio is higher than 1 for effectively considering the intermediate longitudinal fastener spacing (a) in the design of CFS built-up columns. To incorporate this trend of decreased column strength with respect to the increase in a/L_{crl} ratio (Figs. 6 and 9), the ratio a/L_{crl} is included in local buckling slenderness calculation, and this is named to be modified local buckling slenderness (λ_{lm}).

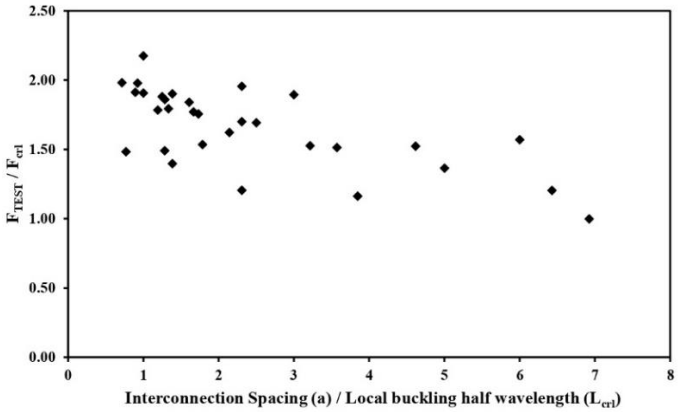

Fig.6. Local buckling stress trend of built-up column with respect to the a/L_{crl} ratio

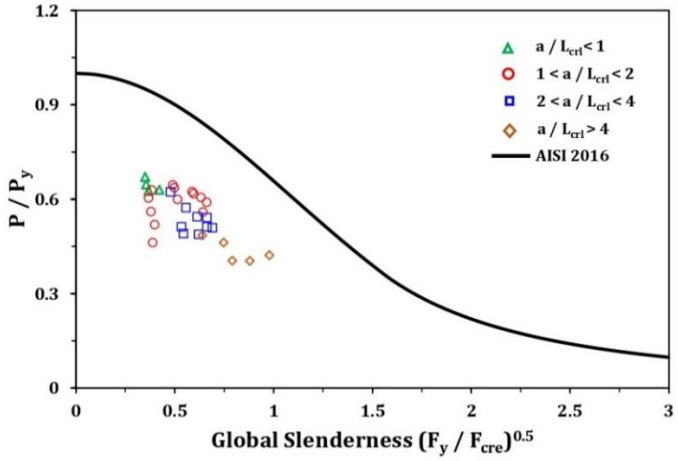

Fig. 7. Comparison of test results with the AISI's global buckling design strength

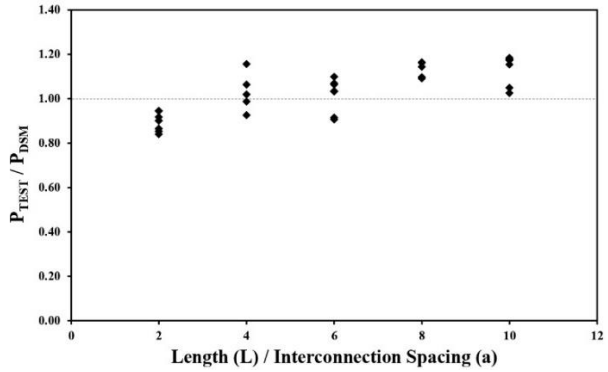

Fig. 8. Test results: local buckling strength trend of built-up column with respect to the L/a ratio

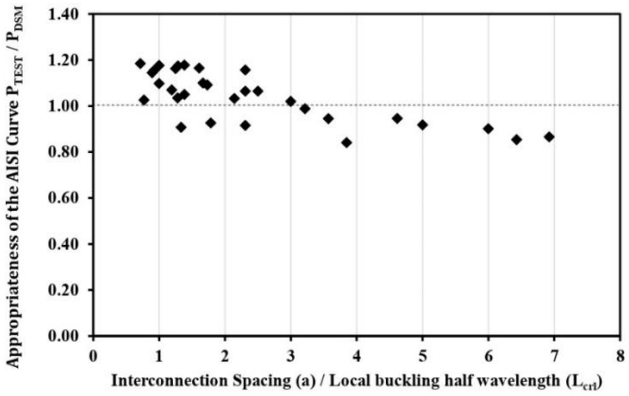

Fig.9. Appropriateness of the AISI local buckling design curve [Eq. (1-3)]

5.Modified Direct Strength Method for CFS face-to-face connected built-up column influenced by intermediate longitudinal fastener spacing (P_{DSM}^{M})

$$P_{nl} = \begin{cases} P_{ne} & if\ \lambda_{lm} \le 0.776 \\ \left[1 - 0.15\left(\frac{1}{\lambda_{lm}^{2}}\right)^{0.4}\right]\left(\frac{1}{\lambda_{lm}^{2}}\right)^{0.4} P_y & if\ \lambda_{lm} > 0.776 \end{cases} \quad (4)$$

$$\lambda_{lm} = \sqrt{\frac{P_{ne}}{P_{crl}}}\left(\frac{a}{L_{crl}}\right)^{0.2} \quad (5)$$

The modified expression for local buckling slenderness expression [Eq. (5)] is included with a/L_{crl} with a power of 0.2. The use of power coefficient 0.2 for a/L_{cr} ratio in the modified slenderness [λ_{lm} - Eq. (5)] ratio will decrease and increase actual local slenderness [λ_l] respectively when the magnitude of a/Lcr ratio is less than 1 and higher than that to appropriately consider the effect of closer fastener spacing and flange overlapping. Similarly, the local buckling design curve of AISI is also modified by replacing the P_{crl}/P_{ne} term with $1/\lambda_{lm}^2$ in Eq. (4). This proposed modified local buckling slenderness is similar to the one proposed by Wang and Young [28].

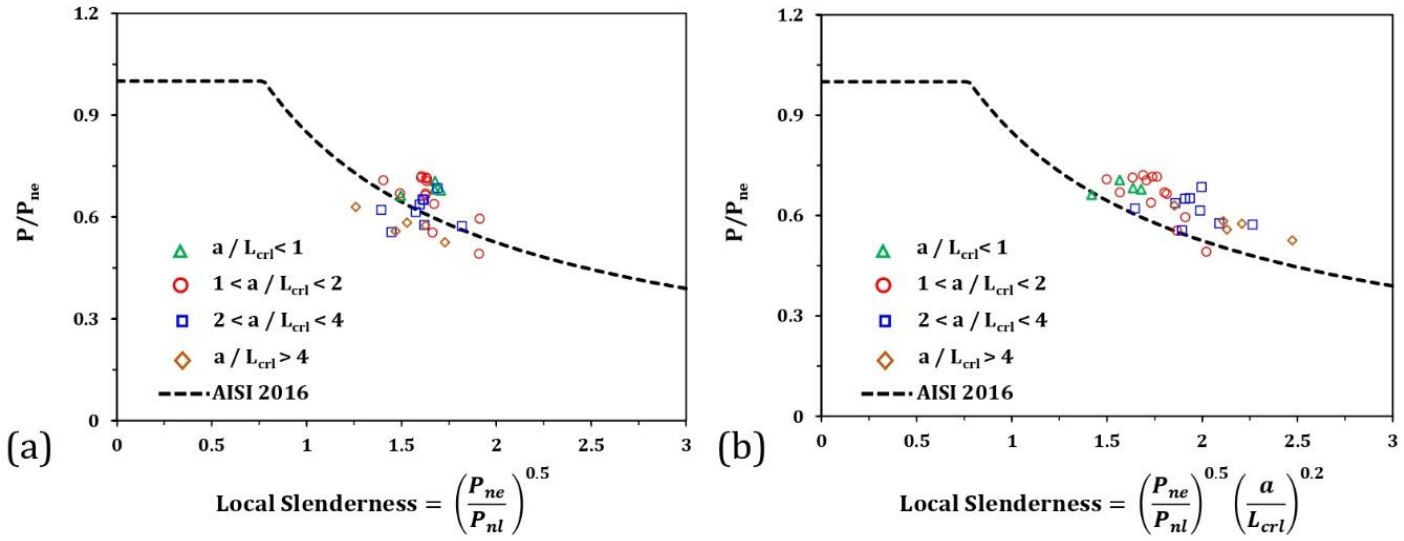

Fig. 10. Comparison between design and test results: (a) Appropriateness of the AISI local buckling design curve [Eq. (1-3)]; (b) Appropriateness of the modified local buckling slenderness ratio approach [Eq. (4-5)]

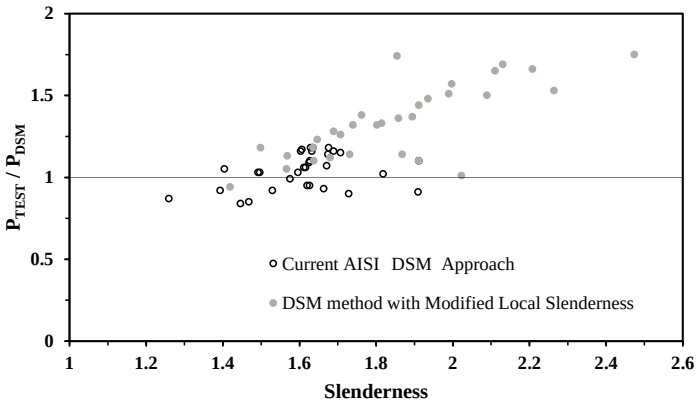

Fig. 11. Comparison between appropriateness of the AISI local buckling design curve [Eq. (1-3)] and modified local buckling slenderness ratio approach [Eq. (4-5)]

The design strength of built-up columns (P_{DSM}^{M}) determined using the modified local buckling slenderness equation [Eq. (5)] is tabulated in Table 2 for direct comparison with the design prediction by current AISI design expressions [P_{DSM} - Eqs. (1-3)] and experimental test results (P_{TEST}). The comparison indicates that the design results using the modified local slenderness are appropriate and conservative for 30 out of 31 built-up columns tested. The values of standard deviation and coefficient of variation are 0.227 and 0.169, respectively, indicating that some design results are having higher conservativeness. It should be noted that such safe design predictions are necessary due to the influence of larger a/L_{crl} ratio (a/L_{crl} ratio 2.5 and beyond). The unconservativeness of the current AISI design method and the conservativeness of the suggested modified local slenderness method are compared in Fig. 10 for easy of understanding. As can be observed from Fig. 10, the local slenderness of the individual channels in the built-up columns increases with an increase in a/L_{crl} ratio using the modified slenderness approach.

6. Reliability Analysis

The reliability analysis was performed for the original DSM and DSM with newly suggested modified local slenderness (λ_{lm}) methods to check the adaptability of them in the design specifications. Two different load combinations were used in the reliability index calculations specified in ASCE [30] and AS/NZS [31] as 1.2 D+1.6 L and 1.2 D + 1.5 L respectively, where D is the dead load and L is the live load. The statistical parameters used (V_f = 0.05, F_m = 1.00, V_m = 0.10 and Mm = 1.1) for the calculation of reliability index is given in Table K2.1.1-1 of AISI [8] and the mean values of P_{TEST} / P_{DSM} and P_{TEST} / P_{DSM}^{M} (P_m) and coefficient of variation values (V_p) for the corresponding design methods are shown in Table 1.

The results of the reliability index calculations indicates that DSM design approach with modified local slenderness is showing better reliability ($\beta 1$ = 3.52 and $\beta 2$ = 3.54 for the P_{TEST} / P_{DSM}^{M} is higher than the target reliability index value βo=2.5) and safe design predictions (mean of P_{TEST} / P_{DSM}^{M} is 1.34) as shown in Table 2. Though the original DSM method's (P_{TEST} / P_{DSM}) reliability index values are higher than the target reliability index, in total 11 out of the 31 test results are unconservative and P_{TEST} / P_{DSM} shows scattered results within a small slenderness range of 1.259 to 1.911 (Fig. 11). While the DSM with modified local slenderness P_{DSM}^{M} shows a traditional trend of the steel design as well as the DSM (overly conservative for the highly slenderness values - Schafer [29]). Therefore, the high mean value of

P_{TEST} / $P_{DSM}{}^{M}$ for the DSM with modified local slenderness approach shall not be considered due to a high scatter rather it is an underprediction due to the higher interconnection spacing and high local slenderness λ_{lm}.

7. Conclusions

An experimental investigation was carried out to examine the effect of intermediate longitudinal fastener spacing on the face-to-face connected built-up columns. A total of 31 built-up columns were tested with different design parameters such as local slenderness (λ_l), global slenderness (λ_c), intermediate longitudinal fastener spacing (a), and length of the column (L). The geometric imperfections were measured using a three-dimensional non-contact scanner and the results were summarized. The experimental results and the failure modes were compared with the current AISI's direct strength method. The following conclusions can be drawn from the experimental tests and design predictions:

1. The columns failed in local buckling without any separation between the built-up cross-section even with a single fastener connection [$(a/r_i) < 0.5\ (KL/r)_m$], therefore, the intermediate longitudinal fastener spacing limitations by the AISI S100 [8] may be revised for face-to-face connected closed cross-section CFS built-up columns.
2. The influence of flange overlapping in local buckling strength of the face-to-face connected built-up columns is demonstrated.
3. The design results indicate that the current AISI's DSM method requires modification to account influence of the fastener connection spacing in local buckling stress.
4. This is a preliminary work towards improving the current AISI CFS built-up column design approach, a modified local buckling slenderness (λ_{lm}) approach is suggested based on the idea proposed in [28].

The suggested modified local buckling slenderness (λ_{lm}) approach is validated only for the limited range of specimens (λ_{lm} values ranging from 1.419 to 2.473), therefore more parametric studies with change in cross-section dimensions, length of the member and with interactive buckling scenarios are required for further evaluation of the DSM using modified local buckling slenderness (λ_{lm}) approach. The improvements in the DSM method with respect to the CFS built-up structural members and intermediate fastener spacing can be expected in near future from the present authors.

References

1. Van der Neut, A. (1969). The interaction of local buckling and column failure of thin-walled compression members. Applied Mechanics (pp. 389-399). Springer, Berlin, Heidelberg.
2. Van der Neut, A. (1973). The sensitivity of thin-walled compression members to column axis imperfection. International Journal of Solids and Structures, 9(8), 999-1011.
3. Dinis, P. B., and Camotim, D. (2019). Proposal to Improve the DSM Design of Cold-Formed Steel Angle Columns: Need, Background, Quality Assessment, and Illustration. Journal of Structural Engineering, 145(8), 04019071.
4. Basaglia, C., and Camotim, D. (2012). Buckling, post-buckling, strength, and DSM design of cold-formed steel continuous lipped channel beams. Journal of structural Engineering, 139(5), 657-668.
5. Pham, C. H., and Hancock, G. J. (2013). Experimental investigation and direct strength design of high-strength, complex C-sections in pure bending. Journal of Structural Engineering, 139(11), 1842-1852.
6. Camotim, D., and Basaglia, C. (2014). On the behaviour, failure and direct strength design of thin-walled steel structural systems. Thin-Walled Structures, 81, 50-66
7. Dabaon, M., Ellobody, E. and Ramzy, K., 2015. Nonlinear behaviour of built-up cold-formed steel section battened columns. Journal of Constructional Steel Research, 110, pp.16-28.
8. AISI. (American Iron and Steel Institute) (2016). "North American Cold-Formed Steel Specification for the Design of Cold-Formed Steel Structural Members." AISI-S100-16C, Washington, DC.
9. EN 1993-1-5: Eurocode 3: Design of steel structures, Part 1–5: plated structural elements, European Committee for Standardisation, Brussels, Belgium, 2006.
10. Standards Australia (2018). "AS/NZS 4600:2018, Cold-Formed Steel Structures" Standards Australia/ Standards New Zealand.
11. Selvaraj, S., and Madhavan, M. (2019). Structural design of cold-formed steel face-to-face connected built-up beams using direct strength method. Journal of Constructional Steel Research, 160, 613-628.
12. Selvaraj, S., and Madhavan, M. (2020). Design of cold-formed steel built-up columns subjected to local-global interactive buckling using direct strength method. Thin walled Structures, https://doi.org/10.1016/j.tws.2020.107305.
13. Selvaraj, S. and Madhavan, M., (2021). Direct Strength Approach for Local Buckling of Cold-Formed Steel Built-Up Beams with Slender Unstiffened Flange Elements.

Practice Periodical on Structural Design and Construction, 26(3), p.06021004.

14. Selvaraj, S. and Madhavan, M., (2021). Design of Cold-Formed Steel Back-To-Back Connected Built-up Beams. Journal of Constructional Steel Research, 181, p.106623.
15. Selvaraj, S. and Madhavan, M., 2018. Retrofitting of structural steel channel sections using cold-formed steel encasing channels. Journal of Performance of Constructed Facilities, 32(4), p.04018049.
16. Selvaraj, S. and Madhavan, M., 2022. Experimental investigation and design considerations on cold-formed steel built-up I-section columns subjected to interactive buckling modes. Thin-Walled Structures, 175, p.109262.
17. Selvaraj, S., and Madhavan, M. (2018). Geometric imperfection measurements and validations on cold-formed steel channels using 3D noncontact laser scanner. Journal of Structural Engineering, 144(3), 04018010.
18. Selvaraj, S. and Madhavan, M., (2022). Design of cold-formed steel built-up closed section columns using direct strength method. Thin-Walled Structures, 171, p.108746.
19. Selvaraj, S. and Madhavan, M., (2019), Investigation on sheathing effect and failure modes of gypsum sheathed cold-formed steel wall panels subjected to bending. In Structures (Vol. 17, pp. 87-101). Elsevier.
20. Fratamico, D. C., Torabian, S., Zhao, X., Rasmussen, K. J., and Schafer, B. W. (2018b). Experiments on the global buckling and collapse of built-up cold-formed steel columns. Journal of Constructional Steel Research, 144, 65-80.
21. Padilla-Llano, D., Moen, C.D., Eatherton, M.R., Li, Q., and Bruce, T. (2012) “Compression-Tension Hysteretic Responsee of Cold-Fromed Steel C-Section Framing Members” Proceedings of the 21st International Specialty Conference on Cold-Formed Steel Structures, St. Louis, Missouri, October, 2012.
22. Cardoso, D.C., Harries, K.A. and Batista, E.D.M., (2015). Compressive local buckling of pultruded GFRP I-sections: development and numerical/experimental evaluation of an explicit equation. Journal of Composites for Construction, 19(2), p.04014042.
23. Torabian, S., Zheng, B. and Schafer, B.W., (2015). Experimental response of cold-formed steel lipped channel beam-columns. Thin-walled structures, 89, pp.152-168.
24. Li, Yuanqi; Li, Yinglei; and Song, Yanyong, "Experimental Investigation on Ultimate Capacity of Eccentrically-Compressed Cold-Formed Beam-Columns with Lipped Channel Sections" (2014). International Specialty Conference on Cold-Formed Steel Structures. 3. https://scholarsmine.mst.edu/isccss/22iccfss/session04/3
25. Young, B., 2004. Local buckling and shift of effective centroid of slender sections. Available through: University of Hong Kong [online] website www. hkisc. org/proceedings/2006421/9 Ben-Young. pdf [accessed 19 December 2020].
26. Fratamico, David C.; Torabian, Shahabeddin; Rasmussen, Kim J. R.; and Schafer, Benjamin W., "Experimental Investigation of the Effect of Screw Fastener Spacing on the Local and Distortional Buckling Behavior of Built-Up Cold-Formed Steel Columns" (2016). International Specialty Conference on Cold-Formed Steel Structures. 1. https://scholarsmine.mst.edu/isccss/23iccfss/session8/1.
27. Torabian, S., Chobe, G.S., Crews, J.K. and Schafer, B.W., Stub column response in light of local vs distortional buckling. Proceedings of the Annual Stability Conference Structural Stability Research Council Atlanta, Georgia, April 21-24, 2020.
28. Wang, L. and Young, B., 2018. Behaviour and design of cold-formed steel built-up section beams with different screw arrangements. Thin-Walled Structures, 131, pp.16-32.
29. Schafer, B.W., 2002. Local, distortional, and Euler buckling of thin-walled columns. Journal of structural engineering, 128(3), pp.289-299.
30. ASCE. (2010). Minimum design loads for buildings and other structures. ASCE/SEI 7-10. Reston, VA: ASCE.
31. AS/NZS (Australian/New Zealand Standard). (2002). Structural design actions. Part 0: General principles. AS/NZS 1170.0:2002. Sydney, Australia: Standards Association of Australia.